Oncological hyperthermia: The correct dosing in clinical applications

SUN-YOUNG LEE[1,2], GYULA PETER SZIGETI[3] and ATTILA MARCELL SZASZ[4]

[1]Department of Radiation Oncology, Chonbuk National University Hospital-Chonbuk National University Medical School, Jeonju, Jeonbuk 561-712; [2]Research Institute of Clinical Medicine of Chonbuk National University-Biomedical Research Institute of Chonbuk National University Hospital, Jeonju, Jeonbuk 54907, Republic of Korea; [3]Institute of Human Physiology and Clinical Experimental Research, Semmelweis University; [4]Cancer Center, Semmelweis University, 1083 Budapest, Hungary

Received June 26, 2018; Accepted November 6, 2018

DOI: 10.3892/ijo.2018.4645

Abstract. The problem with the application of conventional hyperthermia in oncology is firmly connected to the dose definition, which conventionally uses the concept of the homogeneous (isothermal) temperature of the target. Its imprecise control and complex evaluation is the primary barrier to the extensive clinical applications. The aim of this study was to show the basis of the problems of the misleading dose concept. A clear clarification of the proper dose concept must begin with the description of the limitations of the present doses in conventional hyperthermia applications. The surmounting of the limits the dose of oncologic hyperthermia has to be based on the applicability of the Eyring transition state theory on thermal effects. In order to avoid the countereffects of thermal homeostasis, the use of precise heating on the nanoscale with highly efficient energy delivery is recommended. The nano-scale heating allows for an energy-based dose to control the process. The main aspects of the method are the following: i) It is not isothermal (no homogeneous heating); ii) malignant cells are heated selectively; and iii) it employs high heating efficacy, with less energy loss. The applied rigorous thermodynamical considerations show the proper terminology and dose concept of hyperthermia, which is based on the energy-absorption (such as in the case of ionizing radiation) instead of the temperature-based ideas. On the whole, according to the present study, the appropriate dose in oncological hyperthermia must use an energy-based concept, as it is well-known in all the ionizing radiation therapies. We propose the use of Gy (J/kg) in cases of non-ionizing radiation (hyperthermia) as well.

Correspondence to: Dr Attila Marcell Szasz, Cancer Center, Semmelweis University, Tomo u. 25-29, 1083 Budapest, Hungary
E-mail: szasz.attila_marcell@med.semmelweis-univ.hu

Key words: hyperthermia dose, CEM43Tx, TRISE, specific absorption rate, modulated electro-hyperthermia

Introduction: Hyperthermia therapy in oncology

Hyperthermia is an ancient method; in fact, it was the very first medical treatment in human medicine. Despite its long history, this approach currently has no widespread applications and is on the periphery of the medical therapies. This contradiction characterizes the history of hyperthermia in medicine.

The use of hyperthermia as a therapy has various stumbling blocks as the effect caused by the absorbed heat is too complex; the applied, absorbed energy is usually depleted non-homogeneously, and the intricacy of biological processes modifies the intended impact of application. The heating process itself represents a further complication: The efficacy indeed differs by the heat source and by the properties of the target volume and its physiological effects. Hyperthermia treatment modalities have yet to progress from a bio-medical experiment to a clinically proven treatment (1,2).

The effect of hyperthermia is not straightforward in *in vivo* experiments and is even more complex in clinical practice. In clinical applications, hyperthermia has two essential effects: i) Thermal damage assessed by the Arrhenius approach and associated evaluations; and ii) physiology-dependent effects are improving the complementary applications.

While the simple thermal effect can be demonstrated using *in vitro* experiments, the evident clinical outcomes are not clearly observable. The challenge is the negative physiological feedback of systemic reactions, which tries to compensate for the increase in temperature and reassert thermal homeostasis.

Hyperthermia is a technically challenging treatment modality. Energy absorption during the heating process entirely depends on the technique applied, and there is no unified protocol for the various technologically determined targets of the heat. The ablation technique differs from the methods causing necrosis or apoptosis, or those that heat up the whole body into the fever range. The category 'hyperthermia' includes the group of energy-absorption methods, and the individual solutions of absorption require an actual protocol. It is very similar in this regard to the chemo-variants of oncological therapies. Chemotherapy, depending on the targets of the drug, has different protocols. Mixing these can

cause severe adverse effects and even fatal events, such as poisoning. Homogeneous targeting in most of these therapies requires very different protocols than local or cell-sensitive selection. For example, chemotherapy is administered intravenously at different doses than with chemoembolization or other types of local administration. Isodose homogeneity, as in radiotherapy, is also not used in most of the brachytherapies, radiation seed or nanoparticle administration. We are sure that the hyperthermia variants also have specific differences in their dose and protocol, sharply depending on their technical solution and targeting method. Defining a general dose and protocol for all hyperthermia methods is a misleading request. The methods are not equal, their effects are different, and thus the dose and protocol have to fit the specific situation.

Oncological hyperthermia suffers presently multiple problems (3), among these the lack of underlying mechanisms of thermal therapies and the missing joint definition of the method and missing a well measurable dose for clinical and research applications.

The choice between thermal or non-thermal and between heat or temperature

The definition of oncological hyperthermia is not unified in the actual literature. The following are a few of the most common definitions found in the literature: i) Hyperthermia is the use of therapeutic heat to treat various types of cancer on and inside the body (4); ii) hyperthermia is the overheating of the body (5); iii) hyperthermia (also known as thermal therapy or thermotherapy) is a type of cancer treatment in which body tissue is exposed to high temperatures [up to 113˚F (45˚C)] (6); iv) hyperthermia therapy is a type of medical treatment in which body tissue is exposed to slightly higher temperatures to damage and kill cancer cells or to render cancer cells more sensitive to the effects of radiation and certain anti-cancer drugs (7); v) hyperthermia involves body temperature which is much higher than normal and is either induced therapeutically or iatrogenically (8); vi) hyperthermia occurs when cells in the body are exposed to temperatures which are higher than normal, and thus changes take place inside the cells (9).

The indefinite definition ranges in a broad spectrum of targets, heating the body, cancer or the malignant cells, and mixes the therapeutic heat and the therapeutic temperature. The key to thermotherapy is the amount and distribution of the absorbed energy in the malignant target. We prefer the definition of oncological hyperthermia as method with which to kill malignant cells by heat-inducing absorbed energy and/or sensitize specific complementary therapies.

The majority of the oncological hyperthermia methods work with absorbed energy by bio-electromagnetic interactions. The biological processes are fundamentally based on the only electromagnetic working ability. Bio-electromagnetic energy exchange is a broad category of energies in life, including all the chemical, mechanical, thermal and bio-electric changes energizing the living processes. The absorption of external energy is necessary for life, it forms an open system; it does not exist in an energetically closed (self-sustaining) mode.

Energy is a global category for all possible work processes. Heat is a type of energy, which can raise the temperature of the target, although not always. An increase in temperature is not the only effect in this complex interaction. The absorbed energy may be utilized for structural rearrangement or chemical reactions, or electromagnetic changes (such as polarization). The temperature strongly depends on how the heat is provided to the system, and how well the system is isolated from its environment. Heat can be transformed into complex changes in the target without an increase in temperature.

A simple example is boiling water. The water reaches its boiling point of 100˚C, and its temperature from that time continually remains at 100˚C; all the heat pumped in is used for evaporation (steam production). The energy is ultimately used to change the structure of the material from solid to liquid.

Temperature is not the heat or even energy of the system. It measures the average energy of the particles in a system. The average does not mean that every particle has the same energy in the equilibrium. The statistical average works differently. For example, the average yearly income in a country does not mean that everyone's salary is the same, and the average does not measure your level of earnings.

Absorbed energy differs from temperature, i.e., the average kinetic energy of particles. A good example is a comparison of warm water in a swimming pool and the same temperature of water in a glass. Heating up the pool needs much more energy than heating up a glass of water to the same temperature. Although heat and temperature are different, these are used equivalently in many instances. The main reason for confusing them is fixed attention to simple situations when the heat does not perform any 'work' in the system's internal energy; it is only homogeneously converted to the average, to the temperature. The energy averaging and characterizing the process by the temperature can happen when we heat clean water between its freezing and boiling points. However, this simple case is very far from the complexity of the living material, which is heterogeneous and uses absorbed heat energy for structural and chemical changes.

Using the temperature like a dose of heating is incorrect; dosing by temperature does not depend on the volume or mass of the target as it is an average and is the same in half or any fraction of the target, while the dose must be different for different sized targets. Due to this, heat is a good candidate for dosing.

Keeping in mind the example of boiling water, holding the temperature at 100˚C while pumping in a massive amount of energy to keep the water boiling is a thermal process, although the temperature does not change. The question thus automatically arises as to what is the proper characteristic that we define as '*thermal*' when the temperature is not a stable indicator of a thermal process. The molecular mechanism of the thermal process defines the probability (reaction rate, k_r) of a jump of a given particle through an energy barrier (activation energy, E_a, measured in J/mol) (Fig. 1).

The energy barrier is mandatory for life processes; without it, an immediate reaction occurs, which explosively drives the reaction out of control. A living system has a funnel-type multibarrier system that gradually loses energy step-by-step during a jump through various reactions in a chain (Fig. 2).

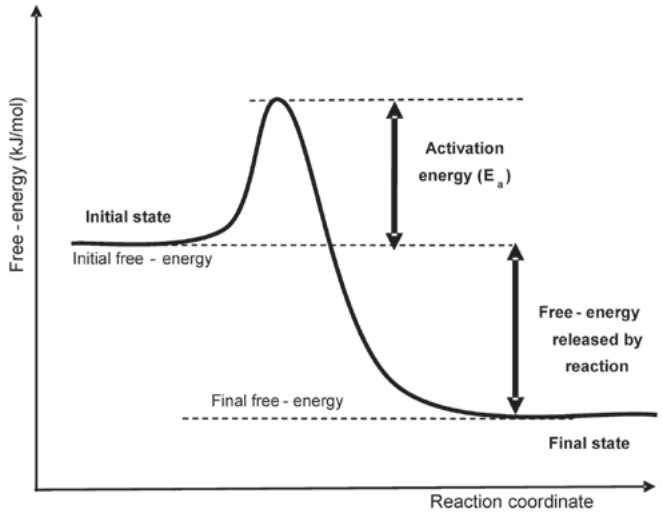

Figure 1. Change in free energy by jumping through an energy barrier (activation energy). The reaction coordinate represents the progress of the chemical reaction pathway. Usually, it describes the geometric changes when a transition happens between particle entities (molecules, atoms, clusters).

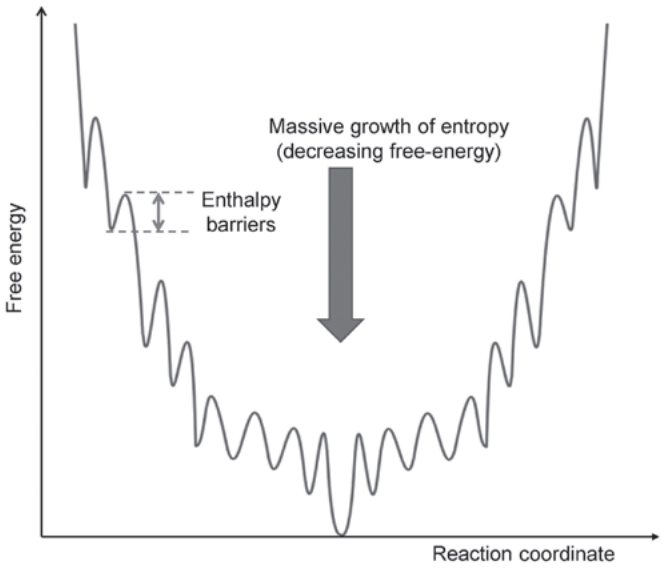

Figure 2. The set of the multiple barriers allowing subsequent small steps of energy-liberation. The 'liberated' energy can provide mechanical work (change height or pressure by lifting, dropping, pumping, etc.), electrical work (change the voltage by ion exchange) or chemical work (change the chemical free energy by the concentration of reactants).

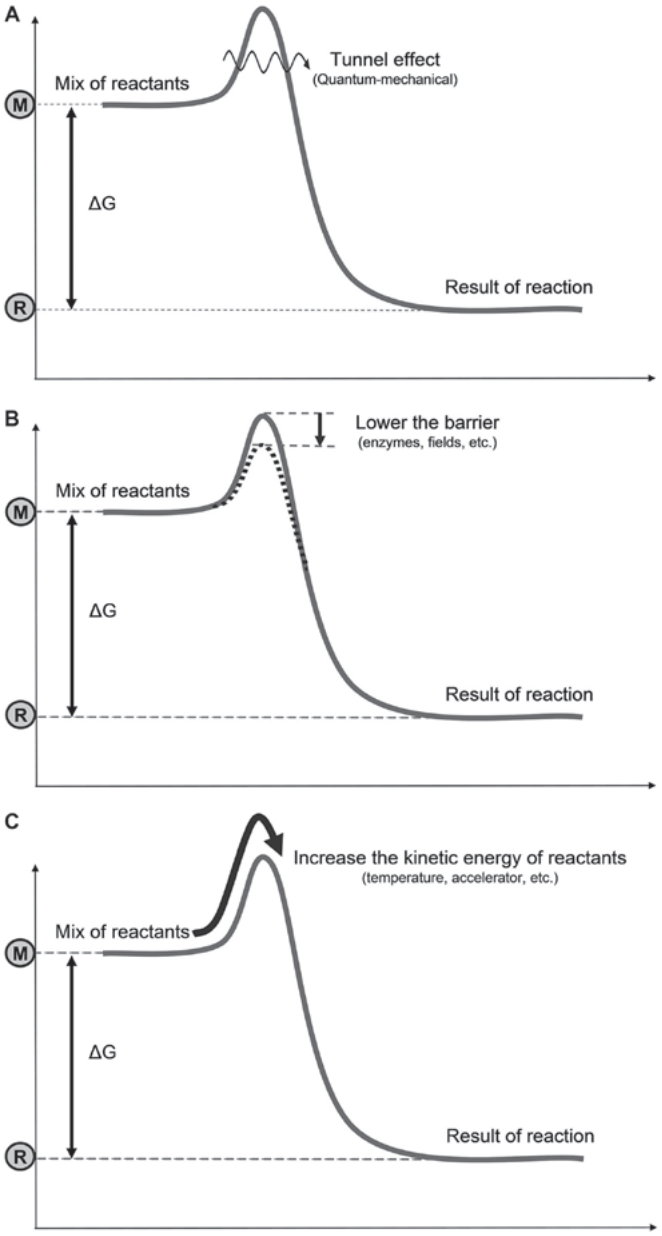

Figure 3. Three processes to go over an energy-barrier: (A) tunneling effect (quantum mechanical), (B) lowering the barrier (catalytic), and (C) reaching the appropriate energy.

Thermal processes are described by an empirical description of the reaction rate, i.e., the Arrhenius equation (10); [Equation 1]:

$$k_r = Ae^{-\frac{E_a}{R_g T}}$$

where T is the absolute temperature, (measured in K), R_g is the universal gas constant

$$(R_g = 8.314 \frac{J}{mol \cdot K})$$

and A is the 'pre-exponential factor' which defines the frequency of collisions, describes the irreversible jump, and measures its dimension in [1/sec]. The Arrhenius equation is an empirical observation, but is precise for most practical applications (11). A detailed history and trends have been described (12).

Three possible mechanisms are available to go over the barrier (Fig. 3): i) Bypass the barrier: A quantum-mechanical (tunneling effect), non-temperature dependent solution (13); destroy or lower the barrier, or form an intermediate compound (transition state); Provide ease for going over the barrier; promoted chemically (e.g., enzymes), electromagnetically (e.g., an electric field), or by other effects; this is a non-temperature dependent solution; iii) surmount the barrier: i.e., A temperature dependent solution by increasing the kinetic energy of the reacting particles, by accelerating

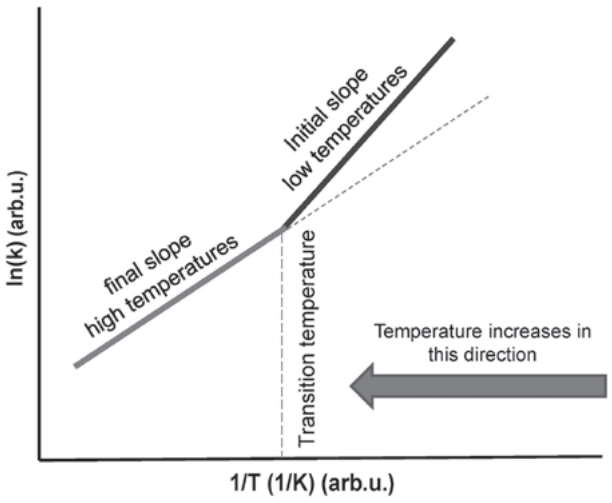

Figure 4. The Arrhenius plot at the transition temperature. The slope of the transition temperature is usually less than that below it, meaning that the new phase at a higher temperature has smaller activation energy. arb.u, arbitrary units.

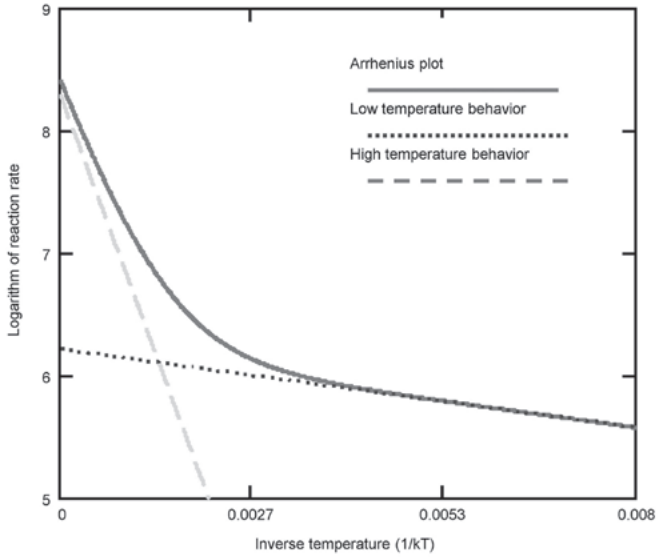

Figure 5. The Arrhenius activation energy can be measured using different methods such as impedance (14).

them individually or increasing their average kinetic energy (temperature). Note that two of these three mechanisms are not temperature-dependent, but are clearly energy consuming; thus, they are thermal.

When a phase transition occurs, the activation energy (E_a) changes and a kink appears on the straight line (Fig. 4). The temperature of the kink is responsible for the transition, and the system remains at this point until the complete transformation has been performed. The kink in the Arrhenius plot is not fixed at a particular temperature, as it may be shifted by various heating processes and by chemotherapy (14) or other chemical conditions (15) that modify the actual reaction (16). An electric field also may affect the kink of the Arrhenius plot (17). The Arrhenius kink, which must be overheated, corresponds well to the believed cellular phase transition observed at around 42.5˚C (18).

When the transition occurs non-homogeneously in the system, then the kink is not a point; it will appear as a curvature on the plot (19,20). The coexistence of two phases could occur for a wide range of temperatures, and then two (or more) Arrhenius lines combine to form the curve (Fig. 5).

When the reaction coordinates change, the system can be approached by the empirical Arrhenius functions. In this case, the process is definitely thermal. Sometimes categories of '*non-thermal*' or '*athermal*' effects are incorrectly used when the process is thermal but non-temperature-dependent.

The internal energy (U) of a system has a substantial variety of physical effects to be changed [Equation 2]:

$$\Delta U = \sum_{\{i\}} Y_i dX_i$$

where Y_i and X_i are thermodynamic variables, intensive and extensive characters of the *i-th* component of the system, respectively. Possible intensive values could be pressure (p), temperature (T), chemical potential (μ), the electric field ($\boldsymbol{E}$) or the magnetic field ($\boldsymbol{H}$), while the extensive values (in order of their pairing with adequate intensives) are the volume (V), the entropy (S), the particle number (N), the polarization ($\boldsymbol{P}$) and the magnetization ($\boldsymbol{M}$). These thermodynamic values add energy terms to the internal energy in individual pairs, and thus the internal energy with some of the interactions is as follows [Equation 3]:

$$\Delta U = p\Delta V - T\Delta S + \mu\Delta N + \boldsymbol{E}\Delta\boldsymbol{P} + \boldsymbol{H}\Delta\boldsymbol{M}$$

This type of non-temperature dependent case occurs in transitions when the internal energy changes at a constant temperature.

Determining the correct the dose of hyperthermia

A well-defined and strictly scientific dose of hyperthermia therapy is a critical issue in research and is crucial to the future of hyperthermia in oncology (21). The proposed general definition of oncologic hyperthermia is forcing cell-damaging energy absorption on malignant cells and sensitizing other therapies. Accordingly, we have to control the damaging thermal effect on malignancy by an appropriate dosing process.

Consequently, the proper dose must be readily applicable to all technical solutions and reliably measured under standard hospital conditions. It must be measured quickly, with acceptable accuracy, and it has to be the basis of the comparison of different treatments by technical variants in clinical practice. The proposed dose at present (22-24) is the cumulative equivalent minutes referring to 43˚C: *CEM43Tx* (measured in minutes). It contains two parts. The *CEM43* part is a time-dependent function *FCEM43˚C(V,t)* [Equation 4]:

$$F_{CEM\,43^{\circ}C}(V,t) = CEM\,43(t) = \int_0^t d\tau\, R^{43-T(\tau)}$$

$$R = \begin{cases} 0.5 \; if \; T \geq 43^{o}C \\ 0.25 \; if \; T < 43^{o}C \end{cases}$$

where V is the volume of the target (the energy is focused on the tumor mass; we assume that only the tumor volume is

heated), t is the time and $T(\tau)$ is the time-dependent temperature, measured in ˚C. The R-value is fixed from the kink of the Arrhenius curve measured by *in vitro* experiments on Chinese hamster ovary cells (25).

The $F_{CEM43^{\circ}C}(V,t)$ function of Eq.4 is extended by a space-time dependent function $T_x(V,t)$, where is the V is the volume of the tumor and x is given in % indicating the average percentage of monitored sensors (V_x portion of the tumor volume) in the V-volume where the temperature is on average $T_x(V,t)$ [Equation 5]:

$$T_x(V,t) = \frac{1}{V_x}\int_0^t\int_{V_x} T(v,\tau)\,dv\,d\tau$$

where V_x is the volume, where the temperature of the monitored sensors on average is $T_x(V,t)$ and thus $x=100V_x/V$ [%].$T_x(V,t)$ is approximated mainly by guessing, and is usually guessed independently of time characterizing the percentage of the tumor which obtains the given minutes by *CEM43˚C*. The missing parameter is real-time mapping, which could change the $T_x(V,t)$ function in real-time, and would be necessary for a correct determination. Due to inhomogenous heat distribution, T_x decreases by growing monitored *volume V*. The dose is finally [Equation 6]:

$$CEM43T_x = F_{CEM43^{\circ}C}(t)\ \text{[min], condition: } T_x(V,t)\ \{[^{\circ}C],[\%]\}$$

which is measured in minutes, but additionally considers the $T_x(V,t)$ conditional function as a reference of *in vitro* necrosis at 43˚C and two other physical units: A unit for the temperature (*K* or ˚C) and a unit for the portion of the isothermal average x (%). For example, $CEM43T_{90}$ measures the cumulative equivalent minutes referring to necrotic cell killing at 43˚C when the measured temperature is actually T_{90} in 90% of the monitored sites (referred to as the thermal isoeffect dose in 90% of the area) (23).

This does use the time in non-conventional units (min instead of sec), and the unit is rigorously somehow a mixture of time and percentage. Non-linear physiological feedbacks need real-time measurements, which are also requested due to the integrative basis of the $CEM43T_x$ dose. Furthermore, this dose value requires registering the temperature distribution of the target in space and time, which is practically not measurable.

Taken together, given the abovementioned challenges, the $CEM43T_x$ dose has another severe scientific problem: The $T(\tau)$ has of course a dimension, ˚*C*. When we measure the temperature in other units (such as ˚*F* or ˚*R*), the value of $CEM43T_x$ will be different if its unit does not contain the unit of the temperature. In the assumed mathematical form, $R^{43-T(\tau)}$ has no dimension, which is not scientifically viable.

Moreover, $CEM43T_x$ is controversial, and has failed to show the local control characterization of clinical results in soft tissue sarcomas (26), but was in line with clinical results for superficial tumors (27). The administered dose of $CEM43T_{90}$ for local hyperthermia did not exhibit an association between dose and clinical outcomes (such as local remissions, local disease-free survival and overall survival) (28). It has been calibrated by *in vitro* experiments (26), which are far from the reality of human medicine. Its necrotic reference at 43˚C renders this dose unrealistic, as in most human hyperthermia treatments such a temperature is not reachable in the whole tumor. While the high temperature is realized in the ablation-like locality, the dosing by $CEM43T_x$ was false (29). The inapplicability of this *in vitro*-calibrated dose is echoed in the whole-body hyperthermia (WBH) application, in which $CEM43T_{100}$ is very high (T_{100} means the complete isothermal heating of the tumor), although the results are very different from the same dose provided by local hyperthermia of the tumor lesion (30).

Sometimes, the dose $CEM43T_x$ is further cumulated by a number of treatments, i.e., 5 repeated treatments of 90 min each, having a different temperature definition, but using T_{90}, which is the average temperature of 90% of the tumor volume (in the case of point sensors, 90% of the sensors) during the 60 min treatment time (31) [Equation 7]:

$$CEM43T_{90} = \sum_{n=1}^{n=5}\int_0^{60} R^{\left(43^{\circ}C-T_{90}(\tau)\right)}d\tau$$

$$R = \begin{cases} 0.5\ if\ T \geq 43^{\circ}C \\ 0.25\ if\ T < 43^{\circ}C \end{cases}$$

The $CEM43T_x$ in general use depends on the number of sessions (N), the duration of the nth session (t_n) and of couse T_x is also time-dependent [Equation 8]:

$$CEM43T_x(N,t_n) = \sum_{n=1}^{N}\int_0^{t_n} R^{\left(43^{o}C-T_x(\tau)\right)}d\tau$$

This cumulation needs to be assessed for the additive effects of the applied sessions independently of their repetition frequency. It is likely that a more extended period between sessions will have a different effect than frequent repetition, due to many changes in the level of stress proteins and the proliferation rate of the remaining living part of the tumor, although these are not considered.

The lack of a consensus on dose is the most substantial blockade to hyperthermia applications. A further challenge is that it is almost impossible to measure among standard conditions; it supposes measuring the temperature. However, the measurements must describe a map of the distribution, which needs many measured points in a tumor. This can be done invasively once. In most publications, the researcher measures the temperature intraluminally near the tumor. This indirect measurement of tumor temperature could skew the whole hyperthermia process. Usually, the intraluminal applications are not precise, as the physiological conditions (mainly the blood-flow) produce different temperature there than in the tumor. Equal energy absorption heats the probe in the lumen to a higher temperature. There is no guarantee that the lumen is heated at the same energy flux as the tumor. Introducing the specific absorption rate (SAR, W/kg) parameter over time (such as in radiation therapy, Gy=J/kg=SAR x time) would be a good dose option. Intensive surface cooling does not allow the correct energy dose; energy, which is taken away by cooling, is missing from the dose. The SAR and the temperature distribution are not identical (32).

There has been a weak attempt to modify the $CEM43T_x$ and its cumulation by introducing the dose *TRISE* (33-35). TRISE is a custom-made thermal dose parameter based

on T50 and the duration of heating, guessing the rise in the average temperature (T_{rise}). TRISE emphasizes the rise in temperature concerning human body temperature. i.e., 37˚C. This supposes that the size of the tumor does not change during the treatment, and the sensors remain in the same positions in the tumor. For example, when the treatment time is unified by every session (90 min), and 5 sessions are in the protocol with the same $\langle T50_n \rangle$ (32), then [Equation 9]:

$$TRISE(90) = \frac{1}{450}\sum_{n=1}^{n=5}(\langle T50_n\rangle - 37°C)\cdot 90 = \frac{1}{5}\sum_{n-1}^{n-5}(\langle T50_n\rangle - 37°C)$$

(using the original notations) [Equation 10]:

$$TRISE = \frac{\sum_{n=1}^{n=max}(ALT50 - 37°C)\times dt}{450}$$

Which is in a generalized form [Equation 11]:

$$TRISE(N,t_n) = T_{rise}(N,t_n) = \frac{1}{N}\sum_{n=1}^{n=N}\frac{(\langle T_{50}(t_n)\rangle - 37°C)}{t_n}\cdot t_n = \frac{1}{N}\sum_{n=1}^{n=N}(\langle T_{50}(t_n)\rangle - 37°C)$$

More preciously [Equation 12]:

$$T_{rise}(N,t_n) = \frac{1}{N}\sum_{n=1}^{N}\int_0^{t_n}\frac{(T_{50}(\tau) - 37^oC)}{t_n}d\tau$$

where '*N*' is the overall number of sessions and '*n*' is the successive number of treatments in the complete cycle of sessions, 't_n' is the duration of the actual n^{th} session, and $\langle T_{50}(\tau)\rangle$ is the actual treatment average over T_x which is the temperature in x=50% of the monitored sites of the target. The average treatment, which covers the part of the target in general x is [Equation 13]:

$$\langle T_x(V,n)\rangle = \frac{1}{V\cdot t_n}\int_V\int_0^{t_n}T_x(v,\tau)dvd\tau \qquad [°C]$$

The $T_{rise}(N,t_n)$ dose (measured in ˚C) is a definite temperature and differs entirely from *CEM43Tx* which is measured in minutes. The temperature is an intensive thermodynamic parameter, which means that it characterizes the thermal situation with an average independent of the mass or volume of the considered system. The temperature is, in the isothermal case, the same in every smaller part of the target, while we expect proportionality of the dose with the volume, i.e., half the volume (mass) would have half the dose. Here again, the possibility of adding subsequent treatments forming an overall dose is entirely missing.

$T_{rise}(N,t_n)$ is approaching the SAR on 50% isothermal area of the tumor, and making great average on the inhomogeneities as well as on the time-variation of the absorbed energy. The correct dose (absorbed energy, A_E) which transforms Eq.(12) scientifically correct and actually optimal [Equation 14]:

$$A_E(N) = \sum_N\int_0^{t_n}(SAR(\tau))d\tau$$

Knowing that [Equation 15]:

$$SAR(t) = c\left(\frac{dT}{dt}\right)$$

In the adiabatic approach the average is [Equation 16]:

$$A_E(N) = c\sum_N\int_0^{t_n}\left(\frac{\Delta T}{t_n}\right)d\tau$$

where ΔT is the temperature increase during the actual session. The Eq.(16) is similar, but more precise than $T_{rise}(N,t_n)$ shown in [Equation 12]. The adiabatic conditions can be ensured by the well selected absorbing volumes and well controlled incident power.

Systemic and local physiological effects introduce inaccuracies to the empirical doses in models *in vivo*, despite some actual measurements in preclinical research, such as a randomized canine trial show the significance of $CEM43T_x$ dose (36). The complete dosing attempts by *CEM43Tx* and *TRISE* are in fact impractical and not applicable in daily practice, and their formulation is far removed from the criteria of scientific requirements for dosing.

The thermal effect

Generally, oncological hyperthermia is the result of energy absorption, which changes the target via chemical, structural, mechanical and electromagnetic variations (the induced anthropogenic fever therapies, or inflammatory local heating by biological effects are not discussed herein). Our topic is limited only for the energy-intake from outside (mostly electromagnetic) sources (37). These processes are constrained and the homeostatic control tries to re-establish the thermal equilibrium by physiological negative feedback effects, mainly by the regulation of vasodilatation. There are some other methods, such as fever production with drugs or biomaterials. However, the physiological mechanisms are opposite than the case by energy absorption; herein, the physiological feedback is positive, inducing the new type of homeostasis. Presently, we deal with only the energy-absorption based hyperthermic methods, which distort malignant cells. Energy absorption changes the temperature of the target in most cases. The temperature can be a tool for restructuring or merely signaling cell death and may orchestrate a complex set of molecules acting systemically against malignancy.

When all the absorbed energy is used for a phase change, the temperature will be fixed during this transition. Defining this effect as 'non-thermal' (38) is an innacuracy. A set of complex thermodynamic and bio-electrodynamic interactions is involved in the process (39), changing various physical characteristics, such as the chemical potential, the entropy, the dipole moments; or they may include in chemical reactions, polarizing molecules, producing an electric current, and so on.

Hyperthermia is a thermal effect on living subjects. Consequently, the Arrhenius function as the basis of the correct dosing (such as was selected for $CEM43T_x$ too) is a perfect choice (22,40). The accurate fitting of experiments to the Arrhenius plot *in vitro* (41,42) is convincing regarding the thermal processes. The *R*-value changes according to the

slopes of the Arrhenius plot. The kink in Arrhenius plot (43), with a sudden change of the slope of the line, is an excellent basis to fit the activation energies below and above the kink at a certain temperature, which provided the value of '*R*' in [Equations 4 and 7]. However, the observed kink is an individual process probably connected to the phase transition. The temperature of the kink is reproducible under the same conditions and same cell line; however, it changes depending on the actual complementary chemotherapy (43,44) or actual cell or tissue (45). Due to the fundamentally complementary applications of hyperthermia, this change in the kink is frequent. The kink is not fixed under preheating conditions (46-49) and it is sensitive to the dynamism of heat transfer as well (50); thus, the *R-value* has to be adjusted to the actual position of the kink.

The kink in the Arrhenius plot is probably a lipid-associated phase transition (50-52), which could lower the activation energy to facilitate changes in the energy provided (53). The change in the kink is expected to be responsive to the blood flow as well (54).

When the kink happens in the Arrhenius plot at T_c temperature, and the activation energies are E_{a1} and E_{a2} above and below it, respectively, then the generalization of R in the CEM-like formulation (55,56) is as follows [Equation 17]:

$$R_{gen} = \begin{pmatrix} e^{-\frac{E_{a1}}{R_g T_c T}} & if \quad T \geq T_c \\ e^{-\frac{E_{a2}}{R_g T_c T}} & if \quad T < T_c \end{pmatrix}$$

where T is the absolute temperature, measured in *K*. When $T \cong T_c$, R_{gen} is constant. We may select T_c as the homeostatic body temperature, *310 K (37˚C)*, as was selected in the *TRISE* proposal. This formulation efficiently introduces generalized cumulative equivalent minutes concerning T_c [Equation 18]:

$$CEM|T_c(t) = \int_0^t d\tau \left(R_{gen}\right)^{(T_c - T(\tau))}$$

When the activation energies are E_{a1} = *365 kcal/mol ≈ 1527 kJ/mol* below this point, while above E_{a2} = *148 kcal/mol ≈ 620 kJ/mol*, below and above the kink point, respectively (18,41), then these values implicate $R_{gen(<43C)}$=*0.159*; $R_{gen(\geq 43C)}$=*0.474*, instead of the widely used $R_{(<43C)}$=*0.25*; $R_{(\geq 43C)}$=*0.5*, respectively. The error is below the robust breakpoint (~36%), indicating that non-necrotic damage cannot be described accurately with the standard *CEM43˚C* dose. In *in vitro* experiments, *x=100%* in the $T_x(V,t)$ function in [Equation 5]. This remarkable deviation occurs as the kink is artificial. The plot is a curvature in reality and depends on the spatial-temporal heterogeneity of the process. Thus, the extrapolated straight line is incorrect in the vicinity of the transition, e.g., the binding of adenosine triphosphate (ATP) to myosin subfragment-1 (46,51) or measuring the cytochrome *c* reductase activity of liver mitochondrial succinate for the heterothermic brown antechinus (57,58).

Making the $CEM|T_c(t)$ value scientifically correct, independent of the measuring units of T temperature [Equation 19]:

$$CEM_{sci}|T_c(t) = \int_0^t d\tau\, Q^{\frac{(T_c - T(\tau))}{T_c}} \qquad \text{where} \qquad Q = \left(R_{gen}\right)^{T_c}$$

Here,

$$\frac{(T_c - T(\tau))}{T_c} = \frac{\Delta T(\tau)}{T_c}$$

is free from the dimension (measuring unit) of the temperature, and Q=constant (when $T \cong Tc$). Due to the high value of temperature in K, but its relatively small difference from T_c in this case [Equation 20]:

$$CEM_{sci}|T_c(t) \approx Q\int_0^t d\tau \left(Q^{-\frac{T(\tau)}{T_c}}\right)$$

The Arrhenius graph gives different time doses for the different points of the target (due to its non-homogeneous structure); this promotes chemical reactions and lowers the activation energy (59). In the case of multiple processes, the so-called 'apparent activation energy' E_{aa} should be introduced (60) [Equation 21]:

$$E_{aa} = R\left(\frac{\partial \ln (k_r)}{\partial \left(\frac{1}{T}\right)}\right)_p$$

When the pre-exponential factor has a temperature independent and temperature dependent part, a constant '*A*' can be separated from the temperature; thus, E_{aa} is the independent part of the temperature, and thus (61) [Equation 22]:

$$k_r = AT^m e^{-\frac{E_{aa}}{R_g T}}$$

In practice, it is a rough linear slope fit on the measured *ln(k)* vs. *(1/T)* function, where a deviation from the slope will refer to differences in the actual chemical reactions. Of note, a complex chemical reaction, such as cooking can be described with such apparent activation energies (62).

The Arrhenius curve is most frequently measured *in vitro*, where necrotic cell death is considered to be the dominant thermal effect under cell culture conditions. In cases of pure thermal necrosis *in vitro*, the cell membrane is lethally damaged [e.g., due to protein denaturation (63)], and the damage point changes the kink of the Arrhenius plot depending on the kind of heating (64). Even the protein folding kinetics exhibit an Arrhenius temperature dependence when corrected for the temperature dependence of protein stability (65) and = transmembrane protein-lipid and protein-protein interactions (66).

The Arrhenius mechanism has a more sophisticated theory, using the variance in the reaction rate by temperature to study the transition phase of the reaction on the energy of the barrier (67,68). In this manner, the semi-empirical Arrhenius equation was rigorously derived from statistical thermodynamics (69), using the enthalpy of activation together with the entropy change in the same process. The transition state of this complex process has been described (20) and further developed (70) for cell death, which approaches practical applications for the thermodynamic description of the multistep complex biological progression of interactions. This rigorous thermodynamic explanation has generalized the thermal dose with improving accuracy possible (71). Eyring and Polanyi (Eyring *et al*, Wynne-Jones and Eyring H, Eyring and Polanyi, Eyring, and Eyring and Stearn) developed a

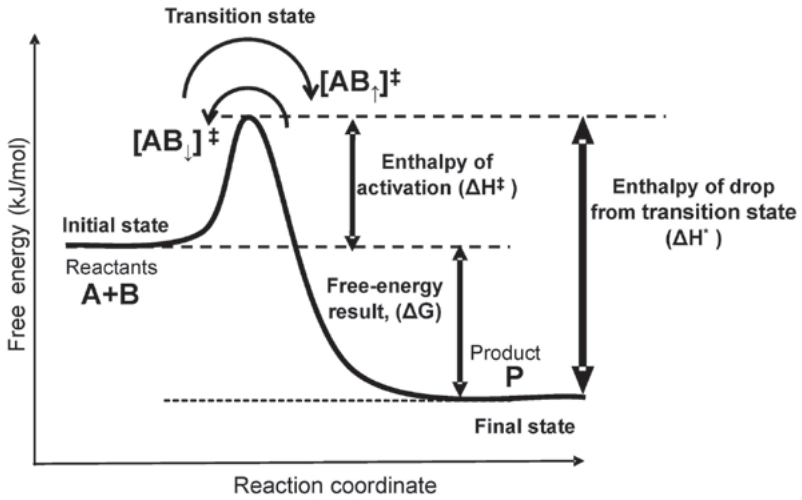

Figure 6. Change in free energy by jumping through an energy barrier (activation energy). 'A' and 'B' are the reactants, 'P' is the product, and the reaction has an intermediate active complex [AB] which has a two-directional probability of proceeding, as most chemical reactions.

theoretically well-supported modification of the Arrhenius plot (68,72-75), which was developed further in Fig. 6 and can be used in quantum-mechanical chemistry (76).

The vital assumption of the transition-state theory is that the transition state is in equilibrium with the reactants and products in the state of the activated complex (11).

The Eyring formulation reforms the reaction coordinates of the conventional empirical Arrhenius plot. The final product develops steadily from the reactant configuration through a transition state. This interim phase is a cluster configuration of the activated transitional complex. In this approach, the reaction coordinate follows the gradient path of potential energy from the initial reactants to the final products, e.g., in simple reactions, the lengths of bonds can be chosen as the reaction coordinate. The transition state population [Equation 23]:

$$k_{tr}^{\#} = \left(\frac{k_B T}{h\upsilon}\right) e^{-\frac{\Delta G^{\#}}{R_g T}}$$

where $\Delta G^{\#}$ is the free energy of activation (transition state), k_B is the Boltzmann's and h is Planck's constant, υ is the vibration frequency of activated complex and $k_{tr}^{\#}$ is the population of the transition state, and the constants are as follows [Equation 24]:

$$k_B = \frac{R_g}{6.022} \cdot 10^{-23} \frac{m^2 kg}{s^2 K} \cong 1.38 \cdot 10^{-23}, h \cong 6.626 \cdot 10^{-34} \frac{m^2 kg}{s}$$

Note that the factor $\left(\frac{k_B T}{h\upsilon}\right)$ is the ratio of the actual thermal and quantum-mechanical energy.

From these, Eyring's expression is formally similar to that of Arrhenius [Equation 25]:

$$k_{tr} = \kappa \left(\frac{k_B T}{h}\right) e^{-\frac{\Delta G^{\#}}{R_g T}}$$

Where 'κ' is the transmission coefficient; it is the probability of oscillation of the activated complex in the transition state leading to a product. The difference, however, is essential: While the Arrhenius plot describes an experimental macroscopic rate constant for the entire transformation process, the Eyring plot deals with microscopic transitions as fundamental steps.

Due to the thermodynamic conditions [Equation 26]:

$$\Delta G^{\#} = \Delta H^{\#} - T\Delta G S^{\#}$$

where $\Delta S^{\#}$ and $\Delta H^{\#}$ are the entropy and enthalpy of activation. For simplicity, we use the molar values of the extensive thermodynamic parameters [Equation 27]:

$$G^{\ddagger} = \frac{G^{\#}}{R_g};\ H^{\ddagger} = \frac{H^{\#}}{R_g};\ S^{\ddagger} = \frac{S^{\#}}{R_g}$$

Using [Equations 25 and 26], we get the following [Equation 28]:

$$k_{tr} = \left(\frac{k_B T}{h}\right) e^{\Delta S^{\ddagger}} e^{-\frac{\Delta H^{\ddagger}}{T}}$$

A comparison of [Equations 28 with 1] makes the pre-exponential frequency factor and the activation energy in empirical Arrhenius function scientifically accurate [Equation 29]:

$$A = \left(\frac{k_B T}{h}\right) e^{\Delta S^{\ddagger}}, \qquad E_a = R_g \Delta H^{\ddagger} = \Delta H^{\#}$$

This result provides an essential explanation for the theoretical background of the pre-exponential factor and the activation energy. The $\Delta H^{\ddagger}$ enthalpy is the kind of energy manifested in a transition state, while the $\Delta S^{\ddagger}$ entropy represents the energy 'trapped' during the interactions.

The Eyring and Arrhenius plots are similar to the fitting of the curves does not differ in the physiological range (77); however, the slope and intercepts have different meanings in Fig. 7. The significant difference is that while the ordinate shows the logarithm of the reaction rate 'k' in the Arrhenius plot, in the Eyring plot, the ordinate has a temperature dependent addition. The superiority of the Eyring model is its theoretical background compared to the empirical Arrhenius model. The central fact that we can use in hyperthermia is that the pre-exponential factor of the Arrhenius plot is entropy

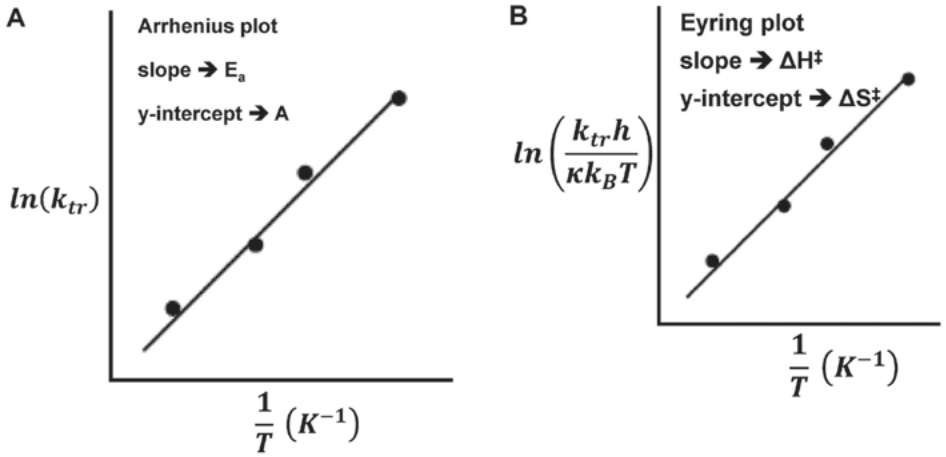

Figure 7. (A) Arrhenius and (B) Eyring plots. The slopes are E_a and $\Delta H^{\ddagger}$ while the y-intercepts are A and $\Delta S^{\ddagger}$, respectively.

dependent. The entropy abruptly jumps during phase transitions, with immediate changes to the chemical structure, which is the essential requirement of hyperthermia.

The Arrhenius parameters (E_a and A) are functionally connected empirically (78) [Equation 30]:

$$E_\alpha \cong 2.61{\cdot}10^3 \ln(A) + 2.62{\cdot}10^4$$

Or [Equation 31]:

$$\ln(A) \cong 3.832{\cdot}10^{-4}\, E_\alpha - 10.042$$

while others (79,80) have slightly different values [Equation 32]:

$$E_\alpha \cong 2.63{\cdot}10^3 \ln(A) + 2.46{\cdot}10^4$$

Or [Equation 33]:

$$\ln(A) \cong 3.8{\cdot}10^{-4}\, E_\alpha - 9.36$$

The linear plots of the Arrhenius parameters [Equations 30, 31, 32, 33) are arithmetically given the same linear dependence of the molar entropy and molar enthalpy due to the Eyring connections, such as seen below:

If, due to [Equation 29] the below are obtained [Equation 34]:

$$E_\alpha = H^{\ddagger} \cong c \ln(A) + \mathrm{d}$$

(c and d are constants) and [Equation 35]:

$$\ln(A) = \frac{S^{\ddagger}}{R_g} + \ln\left(\frac{k_B T}{h}\right) = \frac{S^{\ddagger}}{R_g} + q$$

where q is constant. In consequence [Equation 36]:

$$S^{\ddagger} \cong \left(\frac{R_g}{c}\right) H^{\ddagger} - \left[R_g\left(q + \frac{d}{c}\right)\right] \cong aH^{\ddagger} - b$$

where a and b are constants.

It is indeed observed. A collection of data on molar entropies and enthalpies are found in numerous irreversible thermal denaturalization references; a linear dependence can be seen between the change in molar values (81).

Hence, in case of the processes collected in, the following are obtained [Equation 37]:

$$\Delta S = \alpha \Delta H + b$$

where b=-327.5 [J/mol/K] and a=0.003147 [1/K]; others (82) measure b'=-271.7 [J/mol/K]; a'=0.0030395 [1/K] according to the best fit of the line.

Using the thermodynamical equivalence in [Equation 26] the following are obtained [Equation 38]:

$$\Delta S = \left(\frac{1}{T}\right)\Delta H - \left(\frac{\Delta G}{T}\right)$$

This expression offers the ability to control the accuracy [Equation 39]:

$$T = \left(\frac{1}{a}\right) \cong 317.8[K] \quad \cong 44.6[^{\circ}C]$$

and [Equation 40]:

$$T' = \left(\frac{1}{a'}\right) \cong 329[K] \quad \cong 55.8[^{\circ}C]$$

The above-calculated temperatures fit the experimental conditions. From this, the change in the free energy is as follows [Equation 41]:

$$\Delta G \cong 104{,}067\ [J/mol]$$

and [Equation 42]:

$$\Delta G' \cong 89{,}389\ [J/mol]$$

which is in the range of the usual experimental expectations.

The main consequence of this observation is a clear picture of robustly used energy utilization for chemical changes and differs from the process which leads to an increase in the temperature only.

These processes probably represent different molecular reactions, which require further investigations. This shows that the absorbed energy is utilized for different purposes, not only for raising the temperature. When we intend to change the structure, all the energy components (the chemical reactions, the mechanical properties, and so on) require energy, and the rest will be distributed equally to increase the average kinetic energy of the part of the system. Consequently, the energy that is not used for particular purposes will 'invested into the pool' and will increase the temperature. The increasing temperature represents energy that has no specialized tasks, and thus in this regard, it is wasted energy.

Furthermore, we know another linear expression of molar entropy for the temperature adaptation of enzymes (83) [Equation 43]:

$$\Delta S^{\ddagger} = 4.576\left[ln(K) - 10.753 - ln(T) + \frac{E_a}{4.576T}\right]$$

where and K (sec^{-1}) = (V_{max}/mg of enzyme) x (molecular weight) x (10^{-3} mmol/μmol) x (1 min/60 sec), where the molecular weight of the enzyme is expressed in mg/mmol.

The connections between the activation parameters are observed in cases of muscle-type lactate dehydrogenase, D-glyceraldehyde-3phosphate-dehydrogenase, and muscle glycogen phosphorylase b.

To verify the effect of hyperthermia, thermal damage is measured in multiple experiments. CEM usually characterizes the damage dependent fit to the Arrhenius plot and accurately fits the Arrhenius plot *in vitro* (41,43). According to [Equation 7], the proportional fitting value R depends on the rate of thermal destruction. Since this destruction rate varies according to tissue type, R is not constant at all (84).

Concept: Dose model of modulated electro-hyperthermia

The variability of destruction, as well as the challenge of the previously described competitive effects of thermal damage and blood flow, together with intensified dissemination, need another concept than the pure thermal destruction demonstrated *in vitro*. The thermal process has to be sufficient for the disruption of malignant cells and for sensitizing complementary therapies; however, along with these effects it must not increase the blood flow to a high degree, as this has the deleterious effects of increasing the tumor's nutrient supply and the dissemination of malignant cells, as shown in Fig. 8.

A new type of hyperthermia appears to have solved this challenge: Modulated electro-hyperthermia (mEHT, trade name oncothermia) (79). This method is devoted to using non-temperature dependent thermal effects, which are capable of triggering apoptotic processes by specific molecular processes. We disapprove of the concept of the isothermal heating of the whole tumor mass, avoid the controversial effect which is caused by the feedback of thermal homeostasis, which uses the non-linear control of blood-flow. The energy absorption by the individual malignant cells uses the energy where it is necessary, to initiate apoptotic signal transductions. In consequence, the measured temperature and the stimulated blood-flow are mild (85), but the local control and the overall survival are both increased (86). In this manner, mEHT leads to selective heterogenic heating, genuinely breaking the homogenous, isothermal concept.

The mEHT method uses the biophysical differences between healthy and malignant cells for selection of its action, precisely heating in a nanoscopic range and igniting molecular reactions (87). The selection exploits the character of malignant cells, which indeed differ from their healthy counterparts. Healthy cells are in a communicative network, maintaining the complexity of a well-controlled system, while malignant cells are mostly autonomic, having lost their 'social' connections with other cells, and fighting for with every other cell nutrients, irrespective of their health status. The existence of the network categorizes cells as connected or non-connected (88). Malignant transformation can be regarded as a phase transformation (89), as cells lose their multicellular behavior (90) transforming the highly complex network into a set of individual cells (91,92). This process is similar to reverse evolution (atavism) (93). However, it is different from prokaryotes. These cells are well-developed eukaryotes with complete genetic content, although they have lost their collective complexity, and their mitochondria are not able to supply the enormous energy demand for permanent proliferation.

The consequences of malignant differences indeed provide the possibility to distinguish them from healthy cell arrangements (94). This differentiation is based on the contents of the extracellular aqueous electrolyte. The higher metabolism of malignant cells needs a robust amount of glucose for ATP production, which is measurable by positron emission tomography (95). In cancer cells, ATP production is predominantly performed by simple anaerobic glycolysis instead of mitochondrial phosphorylation. This rapid, intense process produces lactate which, together with the higher transport of other ionic species, considerably increases the ionic conductivity of the electrolyte in the extracellular matrix of the tumor. An applied radiofrequency (RF) current prefers flowing through the low resistance tumor than the healthy environment. This effect is measurable by RF current density imaging (96). The RF current predominantly flows in the extracellular electrolyte. Its energy-absorption creates an active temperature gradient through the membrane (97).

This tumor selection is accompanied by a cellular difference, making the selection microscopic. In the mEHT method, the overall physiologic feedback loops are not promoted by massive general temperature increase of the targeted volume; mEHT functions as mild hyperthermia macroscopically, while it functions as extreme hyperthermia microscopically for malignant cells. Malignant cells are autonomic and break their intercellular communications, i.e., contacts via adherent proteins and junctions mostly vanish. This difference in the structure of the extracellular environment in the near vicinity of cells (98) renders them distinguishable by their dielectric permeability (99,100), for which the applied RF current flow is discriminatory. This is a well-developed diagnostic method (101) that is applied in mammography (102).

Furthermore, the complete pattern of the malignant tissue differs from the pattern of healthy tissue, which is used for pathological image recognition in biopsy samples. The pathological pattern modifies the spatiotemporal interactions of the cells, which is not a static pattern but dynamically acts via intercellular interactions. These dynamic relations produce a noise of homeostatic equilibrium, which is measured as a peculiar signal (103,104). This noise differs in malignancy

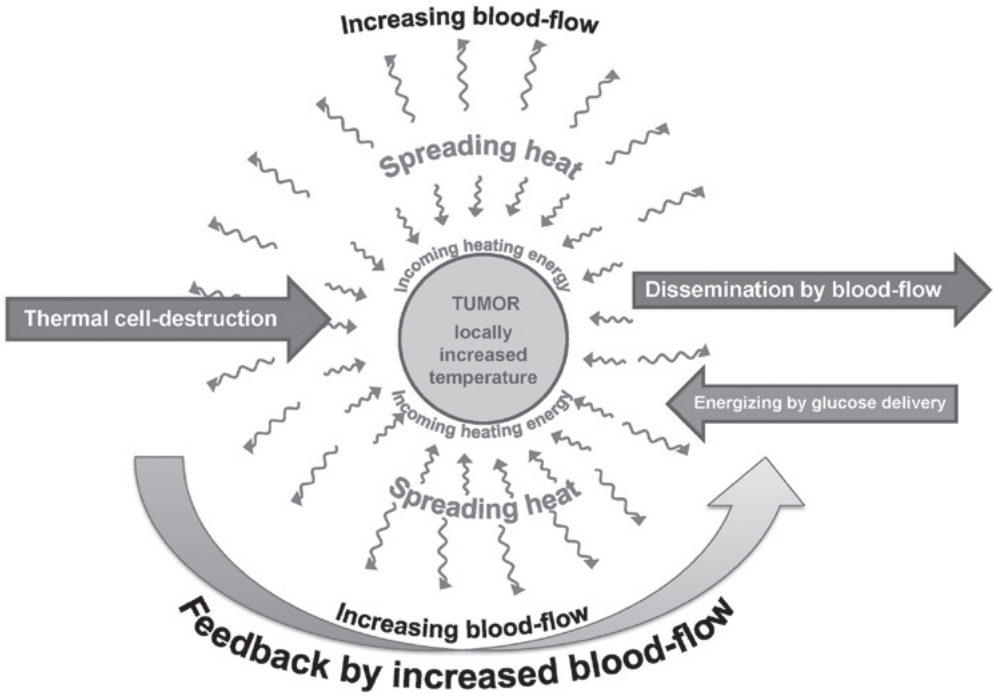

Figure 8. Energy delivery can be well focused, but the heat and the temperature spread. This initiates competitive processes: whether the thermal cell killing, or the tumor-supporting effects are stronger. The control is indefinite. The main risk is compounded by increased tumor cell dissemination, leading to distant micro- and macrometastases.

versus healthy tissue (104) and is measurable by the RF current (105). The noise difference is the basis for the applied modulation on the RF carrier. The modulation is one of the important features of mEHT (oncothermia) method (106). The modulation is an information delivery to the malignant lesion. The applied time-fractal has such autocorrelation time-lags that well fits to the apoptotic excitation processes and also may reconstruct the broken E-cadherin-beta-catenin cellular connections (107), in repeated independent measurement as well (108).

Technically mEHT couples the electromagnetic energy by high-precision impedance matching (patented), which renders such tight coupling similar to it galvanic. Reflection at 150 W incident is <1% (1 W) in the maximal output of oncothermia device. The conventional hyperthermia devices use 10 times more power than mEHT; however, most of that vanishes by various energy losses (radiation to the air, high energy reflection, heating the electronic parts, etc.). Consequently, they must measure the temperature in the target having idea about the absorbed energy there. The innovative tight coupling allows to use the energy as dose of the mEHT treatment (85).

The above-mentioned selection steps guide energy delivery; using β-dispersion involving bound water on the membrane (109,110). The broad range of β-dispersion has a part denoted by δ, (111), which is primarily selective for transmembrane proteins. This effect indices real energy absorption, which happens at clusters of transmembrane proteins (112-114). All these publications above show the excellent selectivity of the mEHT method, acting on the membrane rafts of the malignant cells, while do not harm any healthy cells, having properties which are well distinguishable by the above-described biophysical factors from the malignant cells (87). The mEHT makes the same apoptosis as conventional hyperthermia does but in lower temperatures by 3˚C (115,116), which is the consequence of the absorption of the energy in transmembrane proteins in the rafts.

Selection and energy absorption by a modulated RF current induce cell destruction beyond simple thermal effects. The *in vitro* research shows the absolute differences of mEHT from the conventional heating like water-bath or simple capacitive coupling (108,115). The *in vitro* proven increased efficacy has been supported by *in vivo* research (117) and continues to prove the feasibility in preclinical (118) and clinical applications (119) as well.

The absorbed energy induces a particular apoptotic process in transmembrane proteins (113), which energy is absorbed by the membrane rafts (structure of transmembrane proteins). This energy promotes the extrinsic pathway of apoptosis through the TRAIL-FAS-FADD complex, leading to cleavage of executor caspase-3 and induction of the apoptotic process, as shown in Fig. 9 (120). Additionally, the activation of caspase-8 could trigger intrinsic pathways together with the cell-wide spread of heating energy. These intrinsic pathways include caspase-independent [activate apoptosis-inducing factor (AIF) (121)] and caspase-dependent apoptosis through cytochrome *c* (122). Furthermore, the pro-apoptotic cell death-related gene network (such as EGR1, JUN and CDKN1A) in induced, as well as the cryoprotective gene network (HSPs) (116). Various pathways are united in the final mechanism of action (Fig. 10).

The destruction of the malignant cell is dominantly apoptotic by the above signal excitations (120) developing a damage-associated molecular pattern (DAMP) (121), is the basis of immunogenic cell-death (ICD) (122). These processes prepare antigen recognition cells to produce helper and killer T-cells with direct recognition of the malignant cells over the

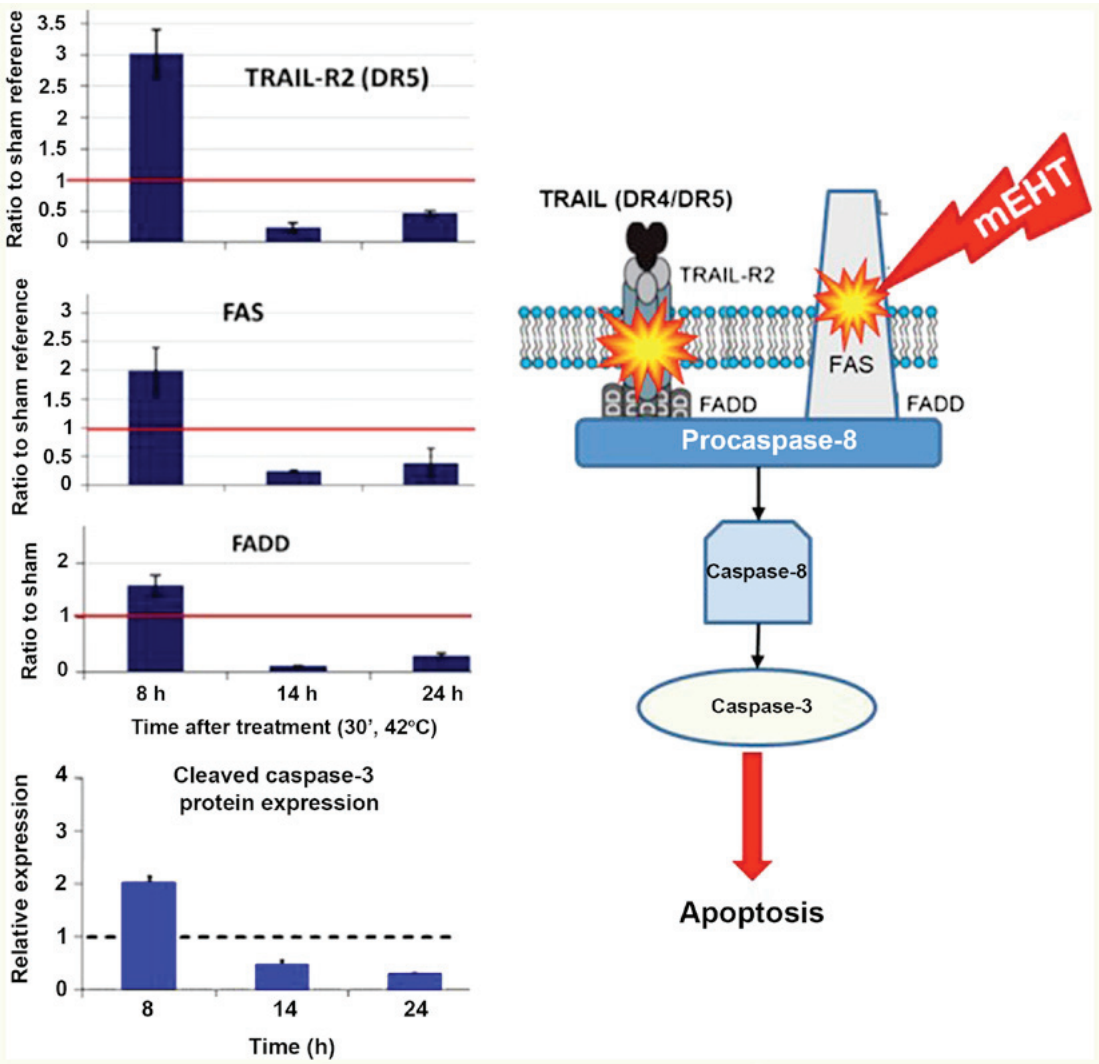

Figure 9. The extrinsic apoptotic pathway induced by mEHT (HT29 human colorectal cell-line in a murine xenograft model) (116,148).

body, finding the disseminated cells and distant metastases, (abscopal effect) (123,124).

This targeting of the extrinsic pathway requires much less energy than heating the complete mass of the tumor, and furthermore, it is a direct apoptosis induction, which is not the case in the isothermal heating. The properly selected energy absorption is the reason why mEHT uses considerably less energy than conventional hyperthermia (125), while its results are showing significant improvement of both the local control and survival time (86).

Thermally activated non-necrotic cell-killing has a point of no return, where the process becomes irreversible, and the cell is committed to die. One of the pathways is BAX-mediated pore formation on mitochondria and the release of cytochrome *c*. Apoptosis and necrotic cell death are complex processes involving numerous chemical reactions and required a long period of time to be completed (126). The apoptotic signals begin the process, which is at the beginning, reversible. There are some points (depending on the signaling pathway) which are the 'points of no return' from where the process automatically continues and finishes by positive feedback constraint. In principle, the final phagocytosis of apoptotic bodies could be 48 h after the process has commenced.

One of the characteristic points of no return is the release of cytochrome *c* from the mitochondria (127), which usually takes 4 h after the initial apoptotic signal. Apparent activation energies associated with protein dynamics show relatively simple straight-line Arrhenius plots, so deviations from the single reaction plot are acceptable (128). In most reactions in living systems, Arrhenius plots are linear (no kink) below 42˚C, e.g., in the mitochondrial membrane (54,129) and BAX-mediated pore formation (130,131) which is connected to cytochrome *c* (132,133), the appearance of which is one of the points of no return. Essential variations in cell polarity (134), enzymatic reactions (135), signaling pathways (136), or the activation of the hsp27/p38MAPK stress pathway (137) could help destroy or modify cancerous tissues.

A single E_{aa} can describe these processes as the kink of the Arrhenius plot is outside the investigated temperature interval. Using the E_{aa} apparent activation energy in complex reaction-kinetic processes of apoptosis can be formally converted to the apparent molar enthalpy and molar entropy. The entropy shows the energy part, which is trapped in the chemical and structural changes caused by the treatment. For dosing, we have to choose a parameter characterizing the process of non-necrotic cell killing.

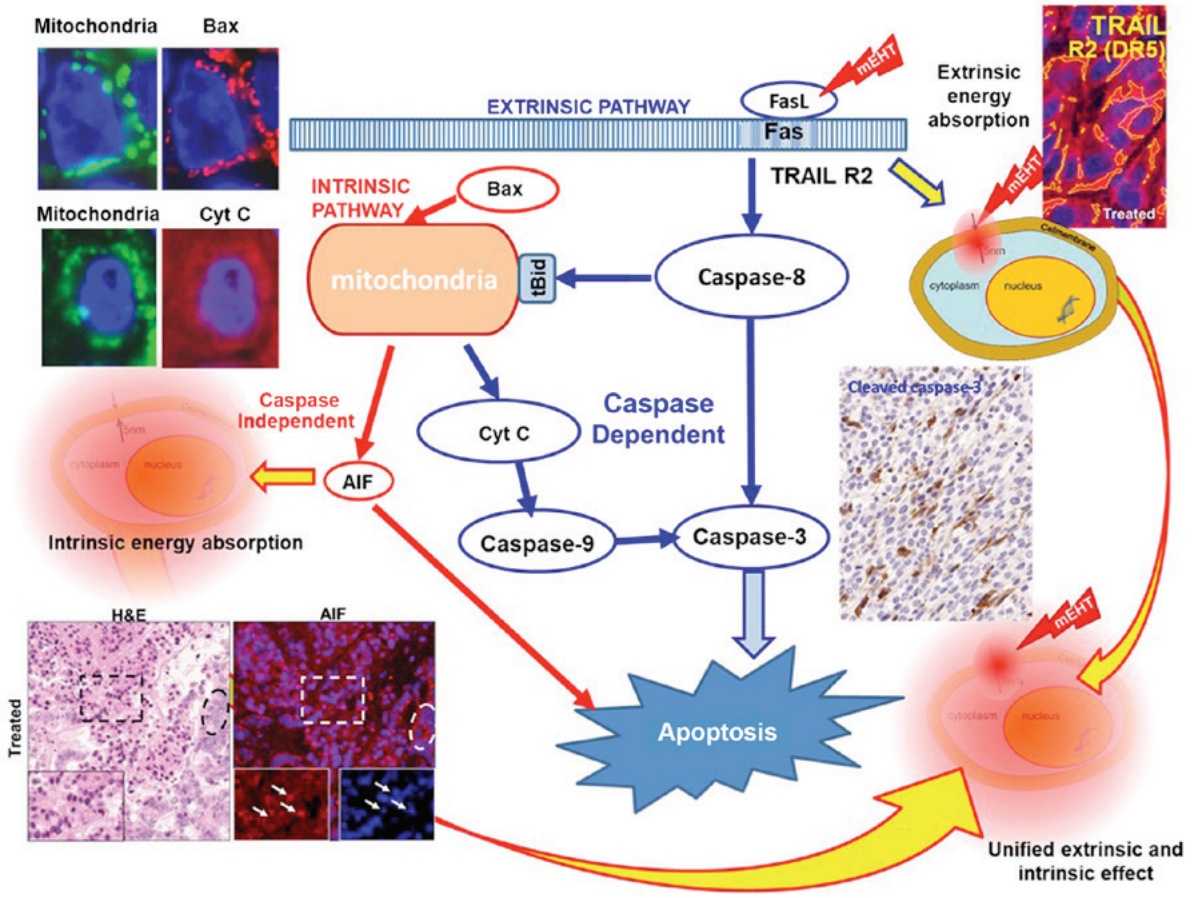

Figure 10. The extrinsic apoptotic pathway induced by mEHT (HT29 human colorectal cell-line in murine xenograft model) (116,121).

The Eyring (Arrhenius experiment) plots show the possibility of the CEM-like behavior of the dose, as indicated earlier (20,55). However, the difference from the flawed CEM43°CT_x is remarkable. No kink is considered in any of the curves of the various temperature dependences of various protein changes, only the slope (molar enthalpy) and molar entropy involved in the pre-exponential factor are used as proposed (20,55). This has specific disadvantages; however, we have to be sure that only apoptosis is characterized, which involves the actually chosen protein and indicates a definite commitment to apoptosis. This protein could be cytochrome *c*, cleaved caspase-3 or AIF. The signal transfer to apoptosis can occur through various ways.

The signal transduction pathways of apoptosis are mixed and produce a defined result. Thus, we have to use the same concept as that used for ionizing radiation. There, we know that the dominant effect breaks the strands of DNA, which anyway follows Arrhenius plot (138). Heat may also break DNA as shown by its Arrhenius behavior (139). With ionizing radiation, no calculations are made regarding the kind of damage (how many and which strands are damaged); the only point is the measurable result, which is proportional to the applied energy. By targeting breaks in DNA, isodose energy is used, assumed that all malignant cells have the same power to destroy their DNA strands. All the other absorbed energy, which makes heat or destroys parts of healthy cells, is regarded as a side-effect. The isodose condition, of course, has many side-effects, as malignant cells are only slightly selected under isodose conditions. The mEHT method enables the more precise selection since the target has self-selection mechanisms orienting the energy to the places where it acts optimally, which is measurable (113,120-122,140). The efficacy of energy delivery also must be optimal, which has been shown for mEHT (125). The mEHT method is highly personalized (55,141) and thus minimizes adverse effects. Consequently, the dose of mEHT could be the same as for ionizing radiation, with the energy defined as J/kg (Gy) or Ws/kg.

The above considerations are valid for single shot treatments. However, this is not sufficient, as clinical applications always use multiple sequential treatments. A series of sessions is applied clinically, so 'fractional heating' can be dosed. This requires clarification regarding the equilibrium of permanent cell death and the fresh round of cell proliferation, as well as the possibility of reverse chemical reactions. This problem overshadows fractional radiotherapy applications (142,143), as the repair of damaged DNA modifies the results of fractional therapy (144). In our fractional treatment method, this problem is less critical as apoptosis induced via the intrinsic and extrinsic ways is complete, no DNA repair is possible, and only the further proliferation of malignant cells leads to regrowth of the tumorous lesion. The critical result is that proliferation is suppressed in cells not destroyed in the target, measured by the Ki67 proliferation index (145).

Taken together with the molecular changes, the treatment capable of sensitizing the tumor to radio- (146) and chemo- (147) therapies, solving the challenge of the significant

and controversial vasodilation induced by the conventional hyperthermia.

In conclusion, the appropriate dose of oncological hyperthermia has to be the well-known energy-based concept, Gy (=J/kg). This dose is appropriate for the complex non-ionizing radiation process and also unites the complete radiation field (together with ionizing radiation) around the same dose control.

Acknowledgements

Not applicable.

Funding

AMS is grateful for the support of the Hungarian Competitiveness and Excellence Program grant (NVKP_16-1-2016-0042).

Availability of data and materials

Not applicable.

Authors' contributions

SYL, GPS and AMS were involved in the conception and design of the study and worked together on drafting, revising and finalizing it. All authors have read and approved the final manuscript.

Ethics approval and consent to participate

Not applicable.

Patient consent for publication

Not applicable.

Competing interest

The authors declare that they have no competing interests.

References

1. Nielsen OS, Horsman M and Overgaard J: A future for hyperthermia in cancer treatment? Eur J Cancer 37: 1587-1589, 2001.
2. van der Zee J: Heating the patient: A promising approach? Ann Oncol 13: 1173-1184, 2002.
3. Roussakow S: The History Of Hyperthermia Rise And Decline. Hindawi Publishing Corporation, Conference Papers in Medicine 2013: 3428027, 2013.
4. Oncology Encyclopedia (2008) MedicineNet, Hyperthermia definition, Answers. http://www.answers.com/topic/hyperthermia. Accessed May 23, 2018.
5. Medicine.net (2008) Hyperthermia definition. http://www.medterms.com/script/main/art.asp?articlekey=3848. Accessed May 23, 2018.
6. National Cancer Institute, Hyperthermia definition. http://www.cancer.gov/about-cancer/treatment/types/surgery/hyperthermia-fact-sheet. Accessed May 23, 2018.
7. Wikipedia, Hyperthermia definition. https://en.wikipedia.org/wiki/Hyperthermia_therapy. Accessed May 23, 2018
8. Medical Dictionary, Hyperthermia definition. http://medical-dictionary.thefreedictionary.com/hyperthermia. Accessed May 23, 2018.
9. The Americal Cancer Society; Hyperthermia definition, http://www.cancer.org/treatment/treatmentsandsideeffects/treatmenttypes/hyperthermia. Accessed May 23, 2018
10. Arrhenius S: On the reaction rate of the inversion of non-refined sugar upon souring. Z Phys Chem 4: 226-248, 1889.
11. Peleg M, Normand MD and Corradini MG: The Arrhenius equation revisited. Crit Rev Food Sci Nutr 52: 830-851, 2012.
12. Pollak E and Talkner P: Reaction rate theory: What it was, where is it today, and where is it going? Chaos 15, 026116, 2005.
13. Thomson WH: Quantum mechanical transition state theory and tunneling corrections. J Chem Phys 110: 4221-4231, 1999.
14. Urano M: Thermochemotherapy: From in vitro and in vivo experiments to potential clinical application. In: Hyperthermia and Oncology. Urano M and Douple E (eds). VSP Utrecht, Tokyo, pp169-204, 1994.
15. Lin R, Chang DC and Lee YK: Study of temperature effect on single-cell fluid-phase endocytosis using micro cell chips and thermoelectric devices; 14th International Conference on Miniaturized Systems for Chemistry and Life Sciences 3-7 October 2010, Groningen, pp962-965, 2010.
16. Rosemeyer H, Körnig E and Seela F: Dextran-linked purine nucleosides as substrates and inhibitors of adenosine deaminase. Eur J Biochem 127: 185-191, 1982.
17. Antov Y, Barbul A, Mantsur H and Korenstein R: Electroendocytosis: Exposure of cells to pulsed low electric fields enhances adsorption and uptake of macromolecules. Biophys J 88: 2206-2223, 2005.
18. Dewey WC, Hopwood LE, Sapareto SA and Gerweck LE: Cellular responses to combinations of hyperthermia and radiation. Radiology 123: 463-474, 1977.
19. O'Neill DP, Peng T, Stiegler P, Mayrhauser U, Koestenbauer S, Tscheliessnigg K and Payne SJ: A three-state mathematical model of hyperthermic cell death. Ann Biomed Eng 39: 570-579, 2011.
20. Szasz A and Vincze G: Dose concept of oncological hyperthermia: Heat-equation considering the cell destruction. J Cancer Res Ther 2: 171-181, 2006.
21. Jones E, Thrall D, Dewhirst MW and Vujaskovic Z: Prospective thermal dosimetry: The key to hyperthermia's future. Int J Hyperthermia 22: 247-253, 2006.
22. Dewhirst MW, Viglianti BL, Lora-Michiels M, Hanson M and Hoopes PJ: Basic principles of thermal dosimetry and thermal thresholds for tissue damage from hyperthermia. Int J Hyperthermia 19: 267-294, 2003.
23. Dewey WC: Arrhenius relationships from the molecule and cell to the clinic. Int J Hyperthermia 10: 457-483, 1994.
24. Perez CA and Sapareto SA: Thermal dose expression in clinical hyperthermia and correlation with tumor response/control. Cancer Res 44 (Suppl 10): 4818s-4825s, 1984.
25. Sapareto SA and Dewey WC: Thermal dose determination in cancer therapy. Int J Radiat Oncol Biol Phys 10: 787-800, 1984.
26. Maguire PD, Samulski TV, Prosnitz LR, Jones EL, Rosner GL, Powers B, Layfield LW, Brizel DM, Scully SP, Harrelson JM, *et al*: A phase II trial testing the thermal dose parameter CEM43 degrees T90 as a predictor of response in soft tissue sarcomas treated with pre-operative thermoradiotherapy. Int J Hyperthermia 17: 283-290, 2001.
27. Dewhirst MW, Vujaskovic Z, Jones E and Thrall D: Re-setting the biologic rationale for thermal therapy. Int J Hyperthermia 21: 779-790, 2005.
28. de Bruijne M, van der Holt B, van Rhoon GC and van der Zee J: Evaluation of CEM43 degrees CT90 thermal dose in superficial hyperthermia: A retrospective analysis. Strahlenther Onkol 186: 436-443, 2010.
29. Assi H: A New CEM43 Thermal Dose Model Based On Vogel-Tammann-Fulcher Behaviour in Thermal Damage Processes. Ryerson University, Toronto, 2009.
30. Thrall DE, Prescott DM, Samulski TV, Rosner GL, Denman DL, Legorreta RL, Dodge RK, Page RL, Cline JM, Lee J, *et al*: Radiation plus local hyperthermia versus radiation plus the combination of local and whole-body hyperthermia in canine sarcomas. Int J Radiat Oncol Biol Phys 34: 1087-1096, 1996.
31. Franckena M: Hyperthermia for the Treatment of Locally Advanced Cervix Cancer. Erasmus University, Rotterdam, 2010.
32. Van der Zee J: Radiotherapy and Hyperthermia in Cervical Cancer, ESTRO/TMH, presentation, Mumbai, March 2, 2005.
33. Franckena M, Fatehi D, de Bruijne M, Canters RA, van Norden Y, Mens JW, van Rhoon GC and van der Zee J: Hyperthermia dose-effect relationship in 420 patients with cervical cancer treated with combined radiotherapy and hyperthermia. Eur J Cancer 45: 1969-1978, 2009.

34. Schooneveldt G, Bakker A, Balidemaj E, Chopra R, Crezee J, Geijsen ED, Hartmann J, Hulshof MC, Kok HP, Paulides MM, *et al*: Thermal dosimetry for bladder hyperthermia treatment. An overview. Int J Hyperthermia 32: 417-433, 2016.
35. Fotopoulou C, Cho CH, Kraetschell R, Gellermann J, Wust P, Lichtenegger W and Sehouli J: Sehoul: Regional abdominal hyperthermia combined with systemic chemotherapy for the treatment of patients with ovarian cancer relapse: Results of a pilot study. Int J Hyp 26: 118-126, 2009.
36. Thrall DE, LaRue SM, Yu D, Samulski T, Sanders L, Case B, Rosner G, Azuma C, Poulson J, Pruitt AF, *et al*: Thermal dose is related to duration of local control in canine sarcomas treated with thermoradiotherapy. Clin Cancer Res 11: 5206-5214, 2005.
37. Blank M and Goodman R: Electromagnetic fields stress living cells. Pathophysiology 16: 71-78, 2009.
38. Giuliani L and Soffritti M: Non-Thermal Effects And Mechanisms Of Interaction Between Electromagnetic Fields and Living Matter. An ICEMS Monograph; National Institute for the Study and Control of Cancer and Environmental Diseases 'Bernardino Ramazzini'. Vol 5. Fidenza Publication, Bologna, 2010.
39. Vincze G and Szasz A: Critical analysis of the thermodynamics of reaction kinetics. J Adv Phys 10: 2538-2559, 2015.
40. Dewey WC: Arrhenius relationships from the molecule and cell to the clinic. Int J Hyperthermia 25: 3-20, 2009.
41. Lindholm CE: Hyperthermia and Radiotherapy. PhD Thesis, Lund University, Malmö, 1992.
42. Hafström L, Rudenstam CM, Blomquist E, Ingvar C, Jönsson PE, Lagerlöf B, Lindholm C, Ringborg U, Westman G and Ostrup L; Swedish Melanoma Study Group: Regional hyperthermic perfusion with melphalan after surgery for recurrent malignant melanoma of the extremities. J Clin Oncol 9: 2091-2094, 1991.
43. Bhowmick P, Coad JE, Bhowmick S, Pryor JL, Larson T, De La Rosette J and Bischof JC: In vitro assessment of the efficacy of thermal therapy in human benign prostatic hyperplasia. Int J Hyperthermia 20: 421-439, 2004.
44. Urano M and Douple E (eds): Chemopotentiation by Hyperthermia. In: Hyperthermia in Oncology. Vol 4. VSP Utrecht, Tokyo, p173, 1994.
45. Digel I, Maggakis-Kelemen Ch, Zerlin KF, Linder P, Kasischke N, Kayser P, Porst D, Temiz Artmann A and Artmann GM: Body temperature-related structural transitions of monotremal and human hemoglobin. Biophys J 91: 3014-3021, 2006.
46. Lindegaard JC: Winner of the Lund Science Award 1992. Thermosensitization induced by step-down heating. A review on heat-induced sensitization to hyperthermia alone or hyperthermia combined with radiation. Int J Hyperthermia 8: 561-586, 1992.
47. van Rijn J, van den Berg J, Wiegant FA and van Wijk R: Time-temperature relationships for step-down heating in normal and thermotolerant cells. Int J Hyperthermia 10: 643-652, 1994.
48. Henle KJ and RotiRoti JL: Response of cultured mammalian cells to hyperthermia. In: Hyperthermia and Oncology. Urano M and Douple E (eds). Vol 1. VSP, Utrecht, Tokyo, pp57-82, 1988.
49. Konings AW: Interaction of heat and radiation in vitro and in vivo. In: Thermo-radiotherapy and Thermo-chemotherapy. Biology, Physiology and Physics. Vol 1. Seegenschmiedt MH, Fessenden P and Vernon CC (eds). Springer Verlag, Berlin, pp89-102, 1995.
50. Hasegawa T, Gu YH, Takahashi T, Hasegawa T and Yamamoto I: Enhancement of hyperthermic effects using rapid heating. In: Thermotherapy for Neoplasia, Inflammation, and Pain. Kosaka M, Sugahara T and Schmidt KL (eds). Springer Verlag, Tokyo-Berlin, pp439-444, 2001.
51. Biosca JA, Travers F and Barman TE: A jump in an Arrhenius plot can be the consequence of a phase transition. The binding of ATP to myosin subfragment 1. FEBS Lett 153: 217-220, 1983.
52. Watson K, Bertoli E and Griffiths DE: Phase transitions in yeast mitochondrial membranes. The effect of temperature on the energies of activation of the respiratory enzymes of *Saccharomyces cerevisiae*. Biochem J 146: 401-407, 1975.
53. Szigeti, GyP, Szasz O and Hegyi G: Personalised dosing of hyperthermia. J Cancer Diagn 1: 107, 2016.
54. Erdmann B, Lang J and Seebass M: Optimization of temperature distributions for regional hyperthermia based on a nonlinear heat transfer model. Ann NY Acad Sci 858: 36-46, 1998.
55. Vincze G, Szasz O and Szasz A: Generalization of the thermal dose of hyperthermia in oncology. Open J Biophys 5: 97-114, 2015.
56. Pearce JA: Comparative analysis of mathematical models of cell death and thermal damage processes. Int J Hyperthermia 29: 262-280, 2013.
57. Geiser F and McMurchie EJ: Arrhenius parameters of mitochondrial membrane respiratory enzymes in relation to thermoregulation in endotherms. J Comp Physiol B 155: 711-715, 1985.
58. Geiser F and McMurchie EJ: Differences in the thermotropic behavior of mitochondrial membrane respiratory enzymes from homeothermic and heterothermic endotherms. J Comp Physiol B 155: 125-133, 1984.
59. Oleson JR: Calderwood SK, Coughlin CT, Dewhirst MW, Gerweck LE, Gibbs FA Jr, Kapp DS: Biological and clinical aspects of hyperthermia in cancer therapy. Am J Clin Oncol 11: 368-380, 1988.
60. Laider KJ: The development of the Arrhenius equation. J Chem Educ 61: 494-498, 1984.
61. Gardiner WC Jr: Temperature dependence of bimolecular gas reaction rates. Acc Chem Res 10: 326-331, 1977.
62. Petrou AL, Roulia M and Tampouris K: The use of the Arrhenius equation in the study of deterioration and of cooking of foods - some scientific and pedagogic aspects. Chem Educ Res And Pract In Eur 3: 87-97, 2002.
63. Qin Z, Balasubramanian SK, Wolkers WF, Pearce JA and Bischof JC: Correlated parameter fit of arrhenius model for thermal denaturation of proteins and cells. Ann Biomed Eng 42: 2392-2404, 2014.
64. Whitney J, Carswell W and Rylander N: Arrhenius parameter determination as a function of heating method and cellular microenvironment based on spatial cell viability analysis. Int J Hyperthermia 29: 281-295, 2013.
65. Scalley ML and Baker D: Protein folding kinetics exhibit an Arrhenius temperature dependence when corrected for the temperature dependence of protein stability. Proc Natl Acad Sci USA 94: 10636-10640, 1997.
66. Abney JR and Owicki JC: Theories of protein-lipid and protein-protein interactions in membranes. In: Progress in Protein-Lipid Interactions. Watts A and de Pont JJ (eds). Vol 1. Elsevier Biomedical Press, Amsterdam, pp1-60, 1985.
67. Evans MG and Polanyi M: Some applications of the transition state method to the calculation of reaction velocities, especially in solution. Trans Faraday Soc 31: 875-894, 1935.
68. Eyring H: The activated complex in chemical reactions. J Chem Phys 3: 107-115, 1935.
69. Laidler KJ and King MC: The development of transition-state theory. J Phys Chem 87: 2657-2664, 1983.
70. McRae DA and Esrick MA: Changes in electrical impedance of skeletal muscle measured during hyperthermia. Int J Hyperthermia 9: 247-261, 1993.
71. Pearce JA: Improving accuracy in arrhenius models of cell death: Adding a temperature-dependent time delay. Transactions of the ASME. J Biomech Eng 137: 121006, 2015.
72. Eyring H, Gershinowitz H and Sun CE: The absolute rate of homogeneous atomic reactions. J Chem Phys 3: 786-796, 1935.
73. Wynne-Jones WF and Eyring H: The absolute rate of reactions in condensed phases. J Chem Phys 3: 492-502, 1935.
74. Eyring H and Polanyi M: Über Einfache Gasreaktionen. Z Phys Chem B 12: 279-311, 1931 (In German).
75. Eyring H and Stearn AE: The application of the theory of absolute reaction rates to proteins. Chem Rev 24: 253-270, 1939.
76. Crawford BL Jr: Quantum Chemistry. By Henry Eyring, John Walter, and George E. Kimball. J Phys Chem 49: 168-168, 1945.
77. Szasz A, Szasz N and Szasz O: Oncothermia - Principles principles and practices. Springer Science, Heidelberg, 2010.
78. Wright NT: On a relationship between the Arrhenius parameters from thermal damage studies. J Biomech Eng 125: 300-304, 2003.
79. He X: Thermostability of biological systems: Fundamentals, challenges, and quantification. Open Biomed Eng J 5: 47-73, 2011.
80. He X and Bischof JC: Quantification of temperature and injury response in thermal therapy and cryosurgery. Crit Rev Biomed Eng 31: 355-422, 2003.
81. Jacques SL: Ratio of entropy to enthalpy in thermal transitions in biological tissues. J Biomed Opt 11: 041108, 2006.
82. Rosenberg B, Kemeny G, Switzer RC and Hamilton TC: Quantitative evidence for protein denaturation as the cause of thermal death. Nature 232: 471-473, 1971.
83. Low PS, Bada JL and Somero GN: Temperature adaptation of enzymes: Roles of the free energy, the enthalpy, and the entropy of activation. Proc Natl Acad Sci USA 70: 430-432, 1973.

84. Pearce JA: Thermal dose models: Irreversible alterations in tissues. In: Physics of Thermal Therapy, Fundamentals and Clinical Applications. Moros EG (ed). CRC Press, Taylor and Francis Group, Boca Raton, FL, 2013.
85. Lee SY, Kim JH, Han YH and Cho DH: The effect of modulated electro-hyperthermia on temperature and blood flow in human cervical carcinoma. Int J Hyperthermia 34: 953-960, 2018.
86. Lee SY, Lee NR, Cho DH and Kim JS: Treatment outcome analysis of chemotherapy combined with modulated electro-hyperthermia compared with chemotherapy alone for recurrent cervical cancer, following irradiation. Oncol Lett 14: 73-78, 2017.
87. Szasz O, Szasz MA, Minnaar C and Szasz A: Heating preciosity: Trends in modern oncological hyperthermia. Open J Biophys 7: 116-144, 2017.
88. Szent-Gyoergyi A: Cell division and cancer. Science 149: 34-37, 1965.
89. Davies PC, Demetrius L and Tuszynski JA: Cancer as a dynamical phase transition. Theor Biol Med Model 8: 30, 2011.
90. Alfarouk KO, Shayoub ME, Muddathir AK, Elhassan GO and Bashir AH: Evolution of tumor metabolism might reflect carcinogenesis as a reverse evolution process (dismantling of multicellularity). Cancers (Basel) 3: 3002-3017, 2011.
91. Greaves M: Evolutionary determinants of cancer. Cancer Discov 5: 806-820, 2015.
92. Bussey KJ, Cisneros LH, Lineweaver CH and Davies PC: Ancestral gene regulatory networks drive cancer. Proc Natl Acad Sci USA 114: 6160-6162, 2015.
93. Davies PC and Lineweaver CH: Cancer tumors as Metazoa 1.0: Tapping genes of ancient ancestors. Phys Biol 8: 015001, 2011.
94. Warburg O: Oxygen, the Creator of Differentiation, Biochemical Energetics. Academic Press, New York, NY, 1966; (Warburg O: The Prime Cause and Prevention of Cancer, Revised lecture at the meeting of the Nobel-Laureates on June 30, 1966 at Lindau, Lake Constance, Germany, 1966).
95. Oehr P, Biersack HJ and Coleman RE (eds). PET and PET-CT in Oncology. Springer Verlag, Berlin, Heidelberg, 2004.
96. Mikac U, Demsar F, Beravs K and Sersa I: Magnetic resonance imaging of alternating electric currents. Magn Reson Imaging 19: 845-856, 2001.
97. Szasz A, Vincze Gy, Szasz O and Szasz N: An energy analysis of extracellular hyperthermia. Electromagn Biol Med 22: 103-115, 2003.
98. Szentgyorgyi A: Bioelectronics: A Study on Cellular Regulations, Defense and Cancer. Academic Press, London, 1968.
99. Foster KR and Schepps JL: Dielectric properties of tumor and normal tissues at radio through microwave frequencies. J Microw Power 16: 107-119, 1981.
100. Blad B and Baldetorp B: Impedance spectra of tumour tissue in comparison with normal tissue; a possible clinical application for electric impedance tomography. Physiol Meas 17 (Suppl 4A): A105-A115, 1996.
101. Babaeizadeh S, Brooks DH and Isaacson D: 3-D electrical impedance tomography for piecewise constant domains with known internal boundaries. IEEE Trans Biomed Eng 54: 2-10, 2007.
102. Scholz B and Anderson R: On electrical impedance scanning - Principles and simulations. Electromedica 68: 35-44, 2000.
103. Musha T and Sawada Y (eds). Physics of the Living Atate. IOS Press, Amsterdam, 1994.
104. West BJ: Fractal Physiology and Chaos in Medicine. World Scientific, London, 1990.
105. Lovelady DC, Richmond TC, Maggi AN, Lo CM and Rabson DA: Distinguishing cancerous from noncancerous cells through analysis of electrical noise. Phys Rev E Stat Nonlin Soft Matter Phys 76: 041908, 2007.
106. Szasz O, Andocs G and Meggyeshazi N: Modulation effect in oncothermia. Hindawi Publishing Corporation Conference Papers in Medicine 2013: e395678, 2013.
107. Szasz A, Szasz N and Szasz O: Oncothermia - Principles and practices. Springer Science, Heidelberg, pp220, 2010.
108. Yang KL, Huang CC, Chi MS, Chiang HC, Wang YS, Andocs G, *et al*: In vitro comparison of conventional hyperthermia and modulated electro-hyperthermia. Oncotarget 7: 84082-84092, 2016.
109. Pethig R: Dielectric properties of biological materials: Biophysical and medical applications. IEEE Transactions on Electrical Insulation E1-19: 453-474, 1984.
110. Schwan HP: Determination of biological impedances. In: Physical Techniques in Biological Research. Vol 6. Academic Press, New York, NY, pp323-406, 1963.
111. Pennock BE and Schwan HP: Further observations on the electrical properties of hemoglobin-bound water. J Phys Chem 73: 2600-2610, 1969.
112. Szasz O and Szasz A: Oncothermia - nano-heating paradigm. J Cancer Sci Ther 6: 4, 2014.
113. Vincze Gy, Szigeti Gy, Andocs G and Szasz A: Nanoheating without artificial nanoparticles. Biol Med (Aligarh) 7: 249, 2015.
114. Szasz A: Electromagnetic effects in nanoscale range. In: Cellular Response to Physical Stress and Therapeutic Applications. Shimizu T and Kondo T (eds). Nova Science Publishers, Inc., Hauppauge, NY, 2013.
115. Andocs G, Rehman MU, Zhao QL, Papp E, Kondo T and Szasz A: Nanoheating without artificial nanoparticles Part II. Experimental support of the nanoheating concept of the modulated electro-hyperthermia method, using U937 cell suspension model. Biol Med (Aligarh) 7: 1-9, 2015.
116. Andocs G, Rehman MU, Zhao QL, Tabuchi Y, Kanamori M and Kondo T: Comparison of biological effects of modulated electro-hyperthermia and conventional heat treatment in human lymphoma U937 cells. Cell Death Discov 2: 16039, 2016.
117. Andocs G, Renner H, Balogh L, Fonyad L, Jakab C and Szasz A: Strong synergy of heat and modulated electro-magnetic field in tumor cell killing, Study of HT29 xenograft tumors in a nude mice model. Strahlenther Onkol 185: 120-126, 2009.
118. Andocs G, Okamoto Y, Osaki T, Tsuka T, Imagawa T, Minami S, Balogh L, Meggyeshazi N and Szasz O: Oncothermia research at preclinical level. Hindawi Publishing Corporation Conference Papers in Medicine 2013: e272467, 2013.
119. Szasz A: Current status of oncothermia therapy for lung cancer. Korean J Thorac Cardiovasc Surg 47: 77-93, 2014.
120. Meggyeshazi N: Studies on modulated electrohyperthermia induced tumor cell death in a colorectal carcinoma model. PhD Theses. Pathological Sciences Doctoral School, Semmelweis University, Budapest, 2015.
121. Meggyeshazi N, Andocs G, Balogh L, Balla P, Kiszner G, Teleki I, Jeney A and Krenacs T: DNA fragmentation and caspase-independent programmed cell death by modulated electrohyperthermia. Strahlenther Onkol 190: 815-822, 2014.
122. Andocs G, Meggyeshazi N, Balogh L, Spisak S, Maros ME, Balla P, Kiszner G, Teleki I, Kovago C and Krenacs T: Upregulation of heat shock proteins and the promotion of damage-associated molecular pattern signals in a colorectal cancer model by modulated electrohyperthermia. Cell Stress Chaperones 20: 37-46, 2015.
123. Qin W, Akutsu Y, Andocs G, Suganami A, Hu X, Yusup G, Komatsu-Akimoto A, Hoshino I, Hanari N, Mori M, *et al*: Modulated electro-hyperthermia enhances dendritic cell therapy through an abscopal effect in mice. Oncol Rep 32: 2373-2379, 2014.
124. Tsang YW, Huang CC, Yang KL, Chi MS, Chiang HC, Wang YS, Andocs G, Szasz A, Li WT and Chi KH: Improving immunological tumor microenvironment using electro-hyperthermia followed by dendritic cell immunotherapy. BMC Cancer 15: 708, 2015.
125. Szasz O and Szasz A: Heating, efficacy and dose of local hyperthermia. Open J Biophys 6: 10-18, 2016.
126. Elmore S: Apoptosis: A review of programmed cell death. Toxicol Pathol 35: 495-516, 2007.
127. Chang LK, Putcha GV, Deshmukh M and Johnson EM Jr: Mitochondrial involvement in the point of no return in neuronal apoptosis. Biochimie 84: 223-231, 2002.
128. Langdon BB, Kastantin M and Schwartz DK: Apparent activation energies associated with protein dynamics on hydrophobic and hydrophilic surfaces. Biophys J 102: 2625-2633, 2012.
129. Melnick RL, Hanson RM and Morris HP: Membranous effects on adenosine triphosphatase activities of mitochondria from rat liver and Morris hepatoma 3924A. Cancer Res 37: 4395-4399, 1977.
130. Kushnareva Y, Andreyev AY, Kuwana T and Newmeyer DD: Bax activation initiates the assembly of a multimeric catalyst that facilitates Bax pore formation in mitochondrial outer membranes. PLoS Biol 10: e1001394, 2012.
131. Pouliquen D, Bellot G, Guihard G, Fichet P, Meflah K and Vallette FM: Mitochondrial membrane permeabilization produced by PTP, Bax and apoptosis: A 1H-NMR relaxation study. Cell Death Differ 13: 301-310, 2006.
132. De Virville JD, Cantrel C, Bousquet AL, Hoffelt M, Tenreiro AM, Vaz Pinto V, Arrabaca JD, Caiveau O, Moreau F and Zachowski A: Homeoviscous and functional adaptations of mitochondrial membranes to growth temperature in soybean seedlings. Plant Cell Environ 25: 1289-1297, 2002.

133. Lenaz G, Sechi AM, Parenti-Castelli G, Landi L and Bertoli E: Activation energies of different mitochondrial enzymes: Breaks in Arrhenius plots of membrane-bound enzymes occur at different temperatures. Biochem Biophys Res Commun 49: 536-542, 1972.
134. Lee M and Vasioukhin V: Cell polarity and cancer - cell and tissue polarity as a non-canonical tumor suppressor. J Cell Sci 121: 1141-1150, 2008.
135. Litovitz TA, Krause D, Penafiel M, Elson EC and Mullins JM: The role of coherence time in the effect of microwaves on ornithine decarboxylase activity. Bioelectromagnetics 14: 395-403, 1993.
136. Kim EK and Choi EJ: Pathological roles of MAPK signaling pathways in human diseases. Biochim Biophys Acta 1802: 396-405, 2010.
137. Leszczynski D, Joenväärä S, Reivinen J and Kuokka R: Non-thermal activation of the hsp27/p38MAPK stress pathway by mobile phone radiation in human endothelial cells: Molecular mechanism for cancer- and blood-brain barrier-related effects. Differentiation 70: 120-129, 2002.
138. Cuesta-López S, Errami J, Falo F and Peyrard M: Can we model DNA at the mesoscale? J Biol Phys 31: 273-301, 2005.
139. Takahashi A, Matsumoto H, Nagayama K, Kitano M, Hirose S, Tanaka H, Mori E, Yamakawa N, Yasumoto J, Yuki K, *et al*: Evidence for the involvement of double-strand breaks in heat-induced cell killing. Cancer Res 64: 8839-8845, 2004.
140. Kim JK, Prasad B and Kim S: Temperature mapping and thermal dose calculation in combined radiation therapy and 13.56 MHz radiofrequency hyperthermia for tumor treatment. Proc. SPIE 10047. Opt Methods Tumor Treat Detect Mech Tech Photodynamic Ther 26: 1004718, 2017.
141. Szasz O, Andocs G and Meggyeshazi N: Oncothermia as Personalized Treatment Option. Hindawi Publishing Corporation Conference Papers in Medicine 2013: e2941364, 2013.
142. Fowler JF: The first James Kirk memorial lecture. What next in fractionated radiotherapy? Br J Cancer 6: 285-300, 1984.
143. Wang JZ, Li XA, D'Souza WD and Stewart RD: Impact of prolonged fraction delivery times on tumor control: A note of caution for intensity-modulated radiation therapy (IMRT). Int J Radiat Oncol Biol Phys 57: 543-552, 2003.
144. Angus SD and Piotrowska MJ: A matter of timing: identifying significant multi-dose radiotherapy improvements by numerical simulation and genetic algorithm search. PLoS One 9: e114098, 2014.
145. Andocs G, Okamoto Y, Kawamoto K, Osaki T, Tsuka T, Imagawa T, Miniami S, Balogh L, Meggyesházi N and Szasz O: Oncothermia basic research at in vivo level. The first results in Japan. Hindawi Publishing Corporation Conference Papers in Medicine 2013: e197328, 2013.
146. Kim W, Kim MS, Kim HJ, Lee E, Jeong JH, Park I, Jeong YK and Jang WI: Role of HIF-1α in response of tumors to a combination of hyperthermia and radiation in vivo. Int J Hyperthermia 28: 1-8, 2017.
147. Lee SY and Kim MG: The effect of modulated electro-hyperthermia on the pharmacokinetic properties of nefopam in healthy volunteers: A randomised, single-dose, crossover open-label study. Int J Hyperthermia 31: 869-874, 2015.
148. Meggyeshazi N, Andocs G and Krenacs T: Programmed cell death induced by modulated electro-hyperthermia. Hindawi Publishing Corporation Conference Papers in Medicine 2013: e187835, 2013.